Am J Transl Res 2025;17(8):5914-5927
www.ajtr.org /ISSN:1943-8141/AJTR0162368

Original Article

Alcohol promoted prostate microbial imbalance in the rat model of prostatitis

Xin Zhu[1*], Ping Xu[2*], Yandong He[1], Wenlong Lu[1], Zhong Wang[1], Feng Liu[1]

[1]Department of Urology, Shanghai Fengxian District Central Hospital, Urology Specialty Alliance of Fengxian District, Shanghai, P. R. China; [2]Department of Nursing, Shanghai Fengxian District Central Hospital, Shanghai, P. R. China. [*]Equal contributors.

Received November 30, 2024; Accepted June 12, 2025; Epub August 15, 2025; Published August 30, 2025

Abstract: Objective: Alcohol may aggravate the clinical symptoms of chronic prostatitis (CP)/chronic pelvic pain syndrome (CPPS), but the molecular mechanism behind this connection have not been fully understood. In our study, we established a rat model of experimental autoimmune prostatitis (EAP) to investigate the impact of alcohol exposure on the changes in prostatic microbiota. Methods: The EAP rat model was established using prostate steroid-binding protein with subsequently administered alcohol exposure. The concentration of alcohol was quantified by a standard alcohol concentration assay. The inflammatory factors were measured through enzyme-linked immunosorbent assay (ELISA). Subsequently, the composition and diversity of the prostate microbiota were analyzed using 16S rRNA gene sequencing data. Results: Elevated levels of inflammatory factors and morphological characteristics of prostate tissue confirmed that the EAP rat model was successfully established. Following alcohol exposure, a significant increase in blood alcohol concentration was observed. Alcohol exposure further exacerbated dysbiosis in prostate microbiota, altering microbial abundance, evenness, and composition in EAP rats. More than 50 metabolic pathways related to biosynthesis, degradation/utilization/assimilation, detoxification, generation of prostate metabolite and energy, macromolecule modification, glycan pathways and metabolic clusters were predicted to be disrupted. Additionally, metabolomics profiling revealed that alcohol impaired pathways such as PWY-6876, PWY-6339, PWY-722, and PWY-5177, which were strongly associated with microbial changes, including *Streptomyces, Oscillospira, Pseudomonas, Lactobacillus*, unidentified-*Clostridiales*, and unclassified-Bacteria. Conclusion: Our findings suggested that alcohol exacerbates prostatitis by disrupting the balance of prostate microbiota. This finding could provide valuable insights for improving the diagnosis and treatment for patients with alcoholic prostatitis.

Keywords: Prostatitis, alcohol, prostate microbiota, experimental autoimmune prostatitis (EAP)

Introduction

Chronic prostatitis is a prevalent disease affecting adult males, particularly those aged 20 to 40 [1, 2]. Studies have shown that the incidence of chronic prostatitis ranges from 10% to 15% [3]. According to clinical presentations, the National Institutes of Health (NIH) categorize prostatitis into 4 types: NIH-I for acute bacterial prostatitis; NIH-II for chronic bacterial prostatitis; NIH-III for chronic prostatitis/chronic pelvic pain syndrome (CP/CPPS); and NIH-IV for asymptomatic inflammatory prostatitis [4]. CP/CPPS had the highest clinical incidence, accounting for 90% to 95% of patients with chronic prostatitis [5]. CP/CPPS is characterized by a complex etiology and persistent symptoms, often leading to sexual dysfunction and mental disorders, which seriously affected the quality of life of the patients [6, 7]. Although the exact pathogenesis of CP/CPPS remains unclear, it may be related to many factors such as infection, neuropathology, autoimmunity.

Alcohol use disorder is a global public health issue, with alcohol intake impacting nearly every organ system and contributing to various inflammatory diseases, such as hepatitis, pancreatitis, and atherosclerosis [8-10]. Epidemiological studies have also shown a strong association between alcohol consumption and an increased prevalence of CP/CPPS [11, 12]. The symptoms of CP/CPPS were typically more severe in this group. Although treatment may alleviate symptoms, they often recur after alcohol intake, leading to repeated medical visits.

This indicated a clear association between alcohol and the onset of CP [13]. Alcohol affects the body's neutrophil's immunity by impairing neutrophil recruitment, reducing pathogen clearance capability, and decreasing neutrophil production [14, 15]. However, the mechanism by which alcohol induces CP/CPPS is not yet fully understood.

Emerging evidence highlights the prostate microbiota as a crucial regulator in the development and progression of prostate-related diseases [16, 17]. Animal studies have shown that long-term alcohol exposure could lead to dysbiosis in the gut microbiota [18], which may contribute to urinary tract dysfunction [19]. Given its role in the urinary tract, the prostate exhibited varying microbial characteristics with changes in pathological states [20]. A stable composition of the prostate and urethral microbiota is essential for maintaining the integrity of the urogenital barrier and immune homeostasis [21]. Under normal physiological conditions, the urogenital microbiota maintained a dynamic equilibrium and formed a symbiotic relationship with the host, carrying out vital biological functions. Our preliminary study indicated a strong correlation between the dysbiosis of the prostate microbiota and the exacerbation of CPPS symptoms. However, the direct impact of alcohol on the prostate microbiota has not been reported to date.

To investigate the mechanism of alcohol-induced prostatitis symptoms, we established an experimental autoimmune prostatitis (EAP) rat model. Subsequently, we assessed the levels of inflammatory factors to evaluate the effects of long-term alcohol exposure on prostate symptoms. Additionally, we examined the alterations in species composition and abundance, diversity and predicted metabolic function of prostatic microbiota by 16s RNA sequencing.

Methods

Animals

A total of 20 male Wistar rats (aged 8-16 weeks) were provided by Shanghai Slack Laboratory Animal Co., Ltd. (Shanghai, China, SCXK (Shanghai) 2022-0004). The rats were housed in the specific pathogen-free (SPF) animal center at Shanghai Chengxi Biotechnology Co., (Use license: SYXK (Shanghai) 2023-0023) (Shanghai, China), maintained at 22±0.5°C with a 12-h light/dark cycle. Rats had free access to standard lab chow and water ad libitum. After a week of acclimatization, the rats were assigned to one of four groups (n = 5 per group): negative control group (Ctrl), experimental autoimmune prostatitis group (EAP), long-term alcohol exposure group (AL), and combined EAP and long-term alcohol exposure (EAP-AL). The animal study was approved by the Institutional Animal Care and Use Committee of Shanghai Chengxi Biotechnology Co., Ltd. (Approval No.: CX0524-08017). The recommendations were strictly followed.

Purification of prostate steroid-binding protein (PSBP)

The purification of PSBP was conducted as previously described [22]. In brief, the rats' prostate tissue was lysed in the lysis buffer with 0.5% TritonX-100 and a protease inhibitor. The lysates were centrifuged at 12,000 g for 30 mins at 4°C. The concentration of PSBP in the supernatant was measured using a BCA kit (cat. ab102536, Abcam). The PSBP concentration was then diluted to 40 mg/mL with PBS buffer (0.1 mol/L, pH7.4) and stored at -80°C for subsequent experiments.

Experimental autoimmune prostatitis (EAP) model

The animal model of EAP was established following previous published procedure [23]. PSBP (40 mg/mL) was emulsified with complete Freund's adjuvant (CFA) (Sigma-Aldrich) at a 1:1 volume ratio. Rats in EAP and EAP-AL groups (n = 10 total) received 0.1 mL of PBSP injected directly into each lobe of the prostate. Ctrl and AL group rats were injected with 0.1 mL of 0.9% saline in the same manner. To prevent infection, all rats received a subcutaneous injection of penicillin (300,000 units/100 g body weight) daily for one week within 24 h after operation. Four weeks later, each rat received subcutaneous booster injections of 0.1 mL of incomplete Freund's adjuvant at 2 points on the ventral and 2 points on the dorsal sides of the rats.

Alcohol exposure

The rats in AL and EAP-AL groups were given ethanol solution following the compulsory drinking procedure [24]. The concentration of

alcohol was gradually increased in the drinking solution each day from 3% to 20% (V/V) in the following sequence: 3%, 5%, 7%, 9%, 11%, 13%, 15% and 20%. The AL and EAP-AL rats were administered alcohol at a dose of 0.0275 ml/g/kg every other day via intubation for 15 consecutive days during puberty. The Ctrl and EAP groups were given water daily. The model was considered successfully established when stable concentration of blood alcohol was achieved. After alcohol exposure, the rats in EAP-AL groups were used to construct the CP/CPPS model by EAP procedure.

Alcohol concentration assay

Blood samples (50 μl) were collected from the rat tail as previously described [25]. Serum was separated within 2 hours and the alcohol concentration was measured using a blood alcohol assay kit (e036-1-1, Nanjing Jiancheng Institute of Bioengineering, Nanjing, China). The samples were mixed immediately, and the absorbance A1 and A2 were measured at 340 nm at 20 seconds and 140 seconds, respectively. The alcohol concentration was calculated using the following formula: Alcohol concentration = $(A2\text{-}A1)_{test}/(A2\text{-}A1)_{standard\ solution}$ * standard solution concentration (mmol/L).

Hematoxylin and eosin (H&E) staining

Prostate tissues were collected following euthanasia by intraperitoneal injection of sodium pentobarbital (200 mg/kg). The H&E staining was performed as previously described [26]. Briefly, the prostate tissues were fixed in 4% paraformaldehyde (PFA) overnight at 4°C. After paraffin embedding, the tissues were sliced into 5 μm sections. The slices were deparaffined and stained with hematoxylin solution for 5 mins, followed by soaking in hydrochloric acid-ethanol solution 5 times, and then rinsed with water. The slices were subsequently stained with eosin for 3 mins. Prior to mounting with neutral balsam, the slices were washed with water, dehydrated with a graded alcohol series (30%, 50%, 70%, 95% and 100%), and cleared in xylene for 4 times. Images were acquired for analysis by using a light microscope.

Enzyme-linked immunosorbent assay (ELISA)

Levels of inflammatory factors were measured using ELISA assay [27]. The prostate tissues were lysed in lysis buffer and centrifugated at 800 g for 20 mins at 4°C. Protein concentration in the supernatant was determined using a BCA kit. The concentration of tumor necrosis factor (TNF)-α, Interleukin (IL)-6 and IL-1β were quantified using rat-specific ELISA kits: TNF-α (No. PT516), IL-6 (No. PI328), and IL-1β (No. PI303), all obtained from Shanghai Beyotime Biotechnology Co., Ltd. (Shanghai, China).

16S rRNA gene sequencing

Total DNA was extracted from rat prostate tissue using the DNeasy@Blood&Tissue kits (Qiagen). The V3-V4 region of bacterial 16S rRNA were amplified using universal primers, and high-throughput sequencing was performed on the Illumina MiSeq platform. Sequencing data were processed using the QIIME2 software. First, the primer sequences were trimmed using *qiime cutadapt trim-paired*, and reads without matched primers were discarded. Subsequently, quality control, denoising, splicing, and removal of chimeric sequences were conducted using *qiime dada2 denoise-paired*. These preprocessing steps were analyzed independently for each library. After denoising all libraries, the amplicon sequence variants (ASVs) feature sequences and ASV tables were merged, and the singletons ASVs were excluded. Sequence length distributions of high-quality reads were analyzed using R scripts. Microbial diversity was assessed using α-diversity and β-diversity matrics. Species richness was measured using observed species index and Chaol index, while community diversity was measured using the Shannon index and Simpson index. The matrix was obtained based on Bray-Curtis distance. Principal coordinate analysis (PCoA) was performed in R to visualize microbial community structure in three-dimensional space. Linear discriminant analysis effect size (LEfSe) was used to identify significantly different bacteria (biomarkers) with Kruskal-Wallis test, and linear discriminant analysis was used to evaluate the influence with Wilcoxon test.

Statistical analysis

All data were presented as the mean ± standard deviation (SD). Statistical analyses were performed using GraphPad Prism software (GraphPad Software, San Diego, CA, USA) and SPSS 25.0 (IBM Corp., Armonk, NY, USA). The Kruskal-Wallis H test was used for multiple

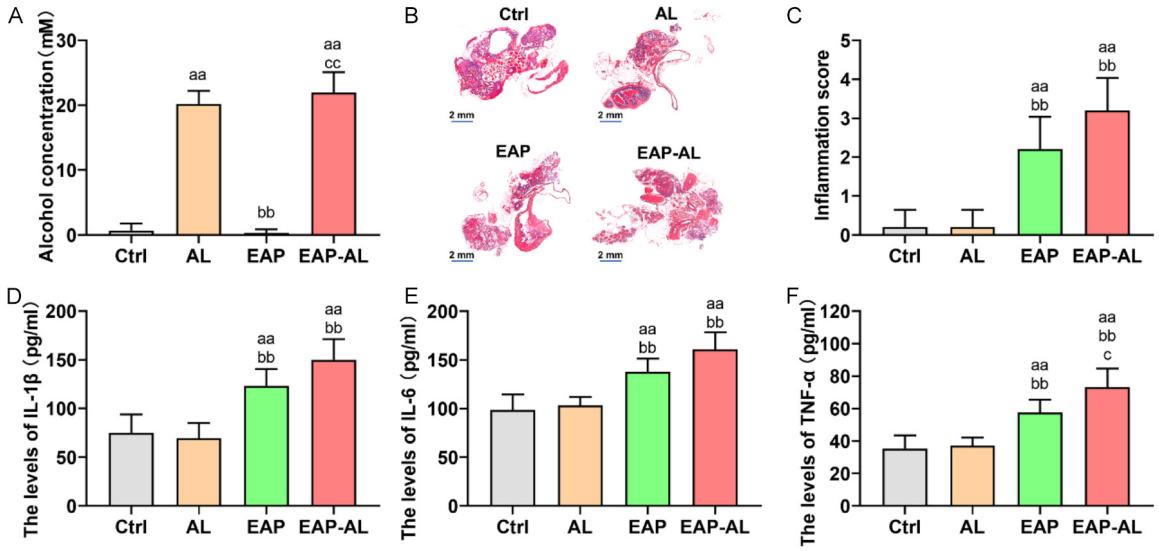

Figure 1. Establishment of EAP and alcohol exposure model in rats. (A) The concentration of alcohol in the blood of rats (n = 5). (B) Representative images of prostate tissue by H&E staining (n = 5). (C) The inflammation scores analysis (n = 5). (D, E) The levels of IL-1β (D), IL-6 (E), and TNF-α (F) in rats by ELISA assay (n = 5). Vs the Ctrl group, $^{aa}P < 0.01$; Vs the AL group, $^{bb}P < 0.01$; Vs the EAP group, $^{c}P < 0.05$, $^{cc}P < 0.01$.

group comparisons. A *P*-value < 0.05 was considered statistically significant.

Results

Establishment of EAP and alcohol exposure rat model

To investigate the effects of EAP and alcohol exposure, we established a rat model following previously reported methods. Blood alcohol concentration was measured to confirm successful alcohol exposure. As shown in **Figure 1A**, the blood alcohol concentration was significantly higher in AL and EAP-AL groups than Ctrl and EAP groups. Histological analysis of prostate tissue using H&E staining revealed no notable inflammation in Ctrl and AL groups. However, we observed that hyperemia, edema, and cell infiltration appeared in the prostatic epithelium and stroma of rats in EAP and EAP-AL groups, with the EAP-AL group showing more severe pathological changes than the EAP group (**Figure 1B**, **1C**). Meanwhile, the levels of IL-1β, IL-6, and TNF-α were further analyzed using ELISA. There was no difference of IL-1β in Ctrl and AL groups, but the levels were markedly elevated in the EAP and EAP-AL groups with the highest level observed in the EAP-AL group (**Figure 1D**). Similarly, IL-6 levels were comparable between the Ctrl and AL groups. There was a significant increase of IL-6 in EAP and EAP-AL groups than in the AL group (**Figure 1E**). No difference of TNF-α was observed between Ctrl and AL groups (**Figure 1F**). TNF-α level was higher in the EAP group compared to the AL group. Interestingly, alcohol further amplified TNF-α levels in EAP rats. Taken together, our results demonstrated that the EAP and alcohol model was successfully established by PBSP and alcohol exposure in rats.

Alcohol promoted prostate microbial dysbiosis in EAP rats

To access the impact of alcohol on prostate microbiota in the context of EAP, we performed 16S rRNA gene sequencing and subsequent bioinformatics analysis. The number of taxa at different structure and characteristics levels were evaluated, including species, genus, family, class, phylum, and domain in the Ctrl, AL, EAP, and EAP-AL groups (**Figure 2A**). The relative abundance of prostate microbiota at family and genus levels were analyzed among four groups. **Figure 2B** showed the differences in prostate microbiota at the phylum level, with Proteobacteria abundance was notably reduced in the EAP and EAP-AL groups compared to the Ctrl and AL groups. The most pronounced decrease was observed in the EAP-AL group. Conversely, Firmicutes and Actinobacteria were significantly enriched in the EAP and EAP-AL groups, and Actinobacteria showing a more

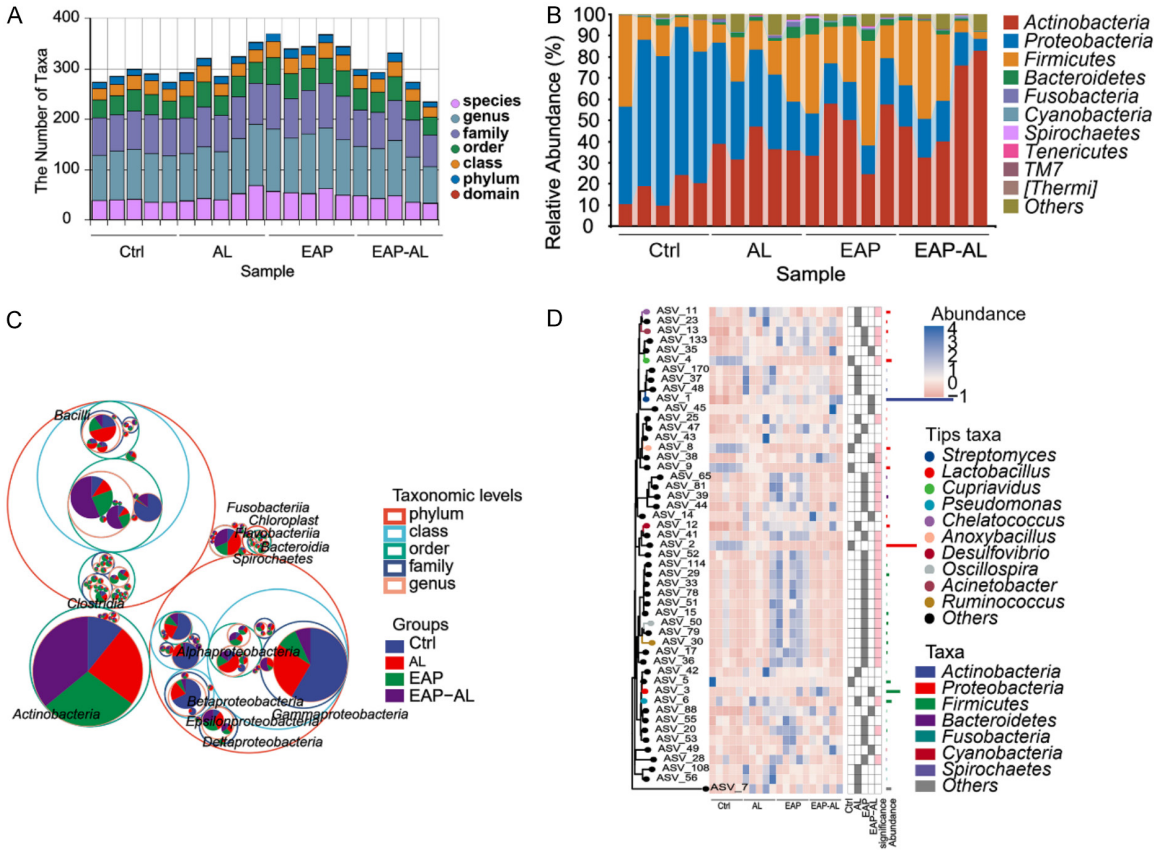

Figure 2. Alcohol promoted the dysbiosis of prostate microbiota in EAP rats. A. The number of taxa of prostate microbiota in rats at different levels, including species, genus, family, class, phylum, and domain. B. The relative abundance analysis at phylum level. C. Taxonomic tree in packed circles for the prostate microbiota at genus, family, class, phylum, and order level of taxa in the four groups. The different colors represented the different taxonomic levels. D. The composition, abundance and taxonomy of prostate microbiota in four groups by phylogenetic tree plot analysis.

dramatical increase in the EAP-AL group. Meanwhile, the results of taxonomic tree in packed circles and phylogenetic tree plot displayed the significant difference in multiple taxonomic levels among the Ctrl, AL, EAP and EAP-AL groups. Notably, changes were observed in Chloroplast, Bacteriodia, Gammaproteobacteria and Betaproteobacteria at phylum level; Alphaproteobacterial and Bacilli at class level; Actinobacteria and Clostridia at order level; Deltaproteobacteria and Epsilonproteobacteria at family level; and Flavobacteriia, Fusobacteridia and Spirochaetes at genus level (**Figure 2C**). Phylogenetic tree analyses further demonstrated significant differences in the relative abundance of Lactobacillus, Shigella, Blautia, Bacteroides, Oscillospira, Dorea, Clostridiaceae_Clostridium, Allobaculum, Ruminococcaceae_Ruminococcus, Paraprevotella, Firmicutes, Bacteroidetes, Proteobacteria, Actinobacteria, Verrucomicrobia and Tenericutes across the four groups (**Figure 2D**). These results suggested that alcohol exacerbates prostate microbiota dysbiosis in EAP rats.

Alcohol alters prostate microbiota composition in EAP rats

To further elucidate the effect of alcohol on prostate microbiota composition in EAP, we compared the microbial diversity among the four groups. The composition of the prostate microbiota within or between different groups were measured by α-diversity and β-diversity analysis. α-diversity metrics, including Chao1, Faith's phylogenetic diversity (PD), Goods coverage, Shannon, Simpson, Pielou-c, and Observed-species indices, were evaluated (**Figure 3A**). Chao1 index showed no significant difference between the Ctrl and AL groups. However,

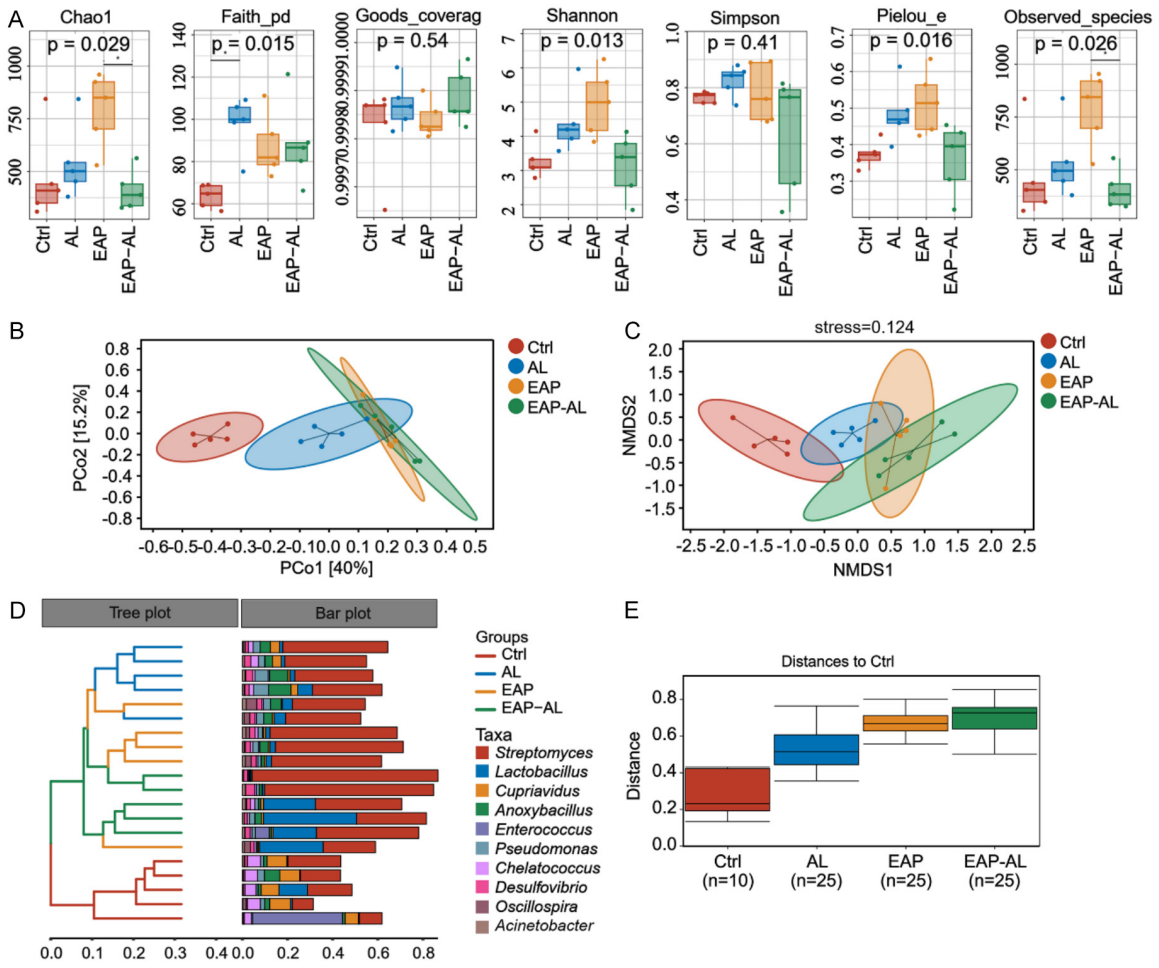

Figure 3. Alcohol changed the diversity of the prostate microbiota in EAP rats. A. The α-diversity analysis of the prostate microbiota at the levels of Chao1, Observed-species, Shannon, Simpson, Faith's PD, Pielou-e, and Goods-coverage. B. The PCoA analysis for distribution characteristics of prostate microbiota. C. The NMDS analysis for distribution characteristics. D. hierarchical clustering analysis for the similarity. E. permutational multivariate analysis for variance; n, the species number of prostate microbiota.

there was a dramatic increase in the EAP group compared with the AL group, while alcohol inhibited the levels of Chao1 in EAP rats. Faith_pd was higher in the AL group relative to the Ctrl group. Goods_coverage remained consistent across all groups. The results of Shannon showed a violent increase in the AL group compared with the Ctrl group, with further elevation in the EAP group, however, the increase was inhibited in the EAP-AL group. No significant difference was observed in the Simpson index among all groups. The level of Pielou-c in AL rats was significantly increased compared to the Ctrl rats. Rats in the EAP group showed that there was dramatically enhanced Pielou-c compared with rats in the AL group, but the level was suppressed by alcohol. Observed-species index showed similar results to Pielou-c.

β-diversity analyses, including PCoA and NMDS, showed distinct clustering patterns among the groups, indicating significant differences in microbial compositions (**Figure 3B**, **3C**). The hierarchical clustering analysis showed similarities between different samples and the top 10 prostate microbiota at genus level, including Streptomyces, Lactobacillus, Cupriavidus, Anoxybacillus, Enterococcus, Pseudomonas, Chelatococcus, Desulfovibrio, Oscillospira, and Acinetobacter (**Figure 3D**). The microbial composition showed high similarity in the Ctrl, AL and EAP groups. Streptomyces and Anoxybacillus were filed in EAP and AL groups, while Lactobacillus was primarily found in the EAP-AL group, and Enterococcus, Chelatococcus and Cupriavidus were in Ctrl group. Permutational multivariate analysis of β-diversity revealed that

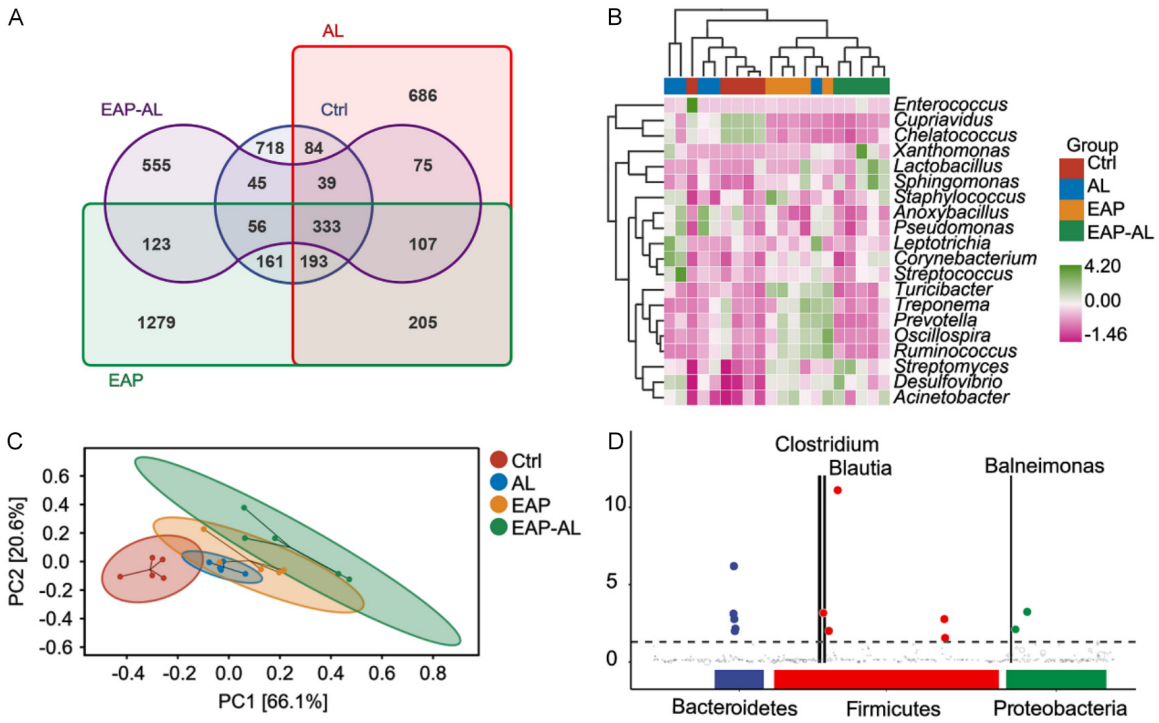

Figure 4. The analysis of marker specie for alcohol exposure in EAP rats. A. Venn diagram analysis of prostate microbiota among four groups. B. Heat map analysis of species composition of the prostate microbiota. C. PCA analysis at the genus level of prostate microbiota. D. The taxonomic distribution of the prostate microbiota by MetagenomeSeq analysis. Significant differences were marked with colored dots or circles, insignificant represented by gray circles, and significantly up-regulated within the group were shown with colored solid dots.

AL, EAP, and EAP-AL rats had a greater microbial community distance from the Ctrl rats. The degree of dissimilarity progressively increased across the AL, EAP and EAP-AL groups (**Figure 3E**). Together, these results indicated that alcohol alters the diversity and composition of the prostate microbiota in EAP rats, potentially contributing to disease progression.

Identification of marker species associated with alcohol exposure in EAP rats

To identify the marker species associated with alcohol exposure in EAP rats, we conducted a comprehensive comparative analysis of prostate microbiota across four groups. The Venn diagram showed a total of 4,659 microbiota were detected across all groups. Specifically, 649 were found in Ctrl and AL groups, 838 in AL and EAP groups, and 619 in EAP and EAP-AL groups. Importantly, 333 prostate microbiota were presented in all groups. While there were 718, 666, 1279 and 555 unique prostate microbiota in Ctrl, AL, EAP, and EAP-AL groups, respectively (**Figure 4A**). The species composition among groups was assessed by using the systematic cluster analysis. The top 20 prostate microbiota at genus level were analyzed based on the heatmap analysis, including Enterococcus, Anoxybacillus, and Pseudomonas (**Figure 4B**). The Enterococcus, Cupriavidus, and Chelatococcus were predominant in the Ctrl group; Anoxybacillus, and Pseudomonas were enriched in the AL group; Turicibacter, Treponema, Prevotella, Oscillospira, Ruminococcus, Streptomyces, Desulfovibrio and Acinetobacter were prominent in the EAP group; and Xanthomonas, Lactobacillus, and Sphingomonas were abundant in the EAP-AL group. Principal component analysis (PCA) further highlighted the differences in microbial communities among the groups. The values of PC1 and PC2 were ranged from -0.5 to -0.1 and -0.3 to 0.2 in the Ctrl group. The AL group showed minimal variation. However, EAP and EAP-AL groups showed broader ranges: PC1 from -0.25 to 0.5 and PC2 from -0.3 to 0.3 in EAP; PC1 from -0.3 to 0.9 and PC2 from 0.55 to 0.75 in the EAPAL group (**Figure 4C**). MetagenomeSeq analysis identified significant differences in the relative abundance of specific taxa among the

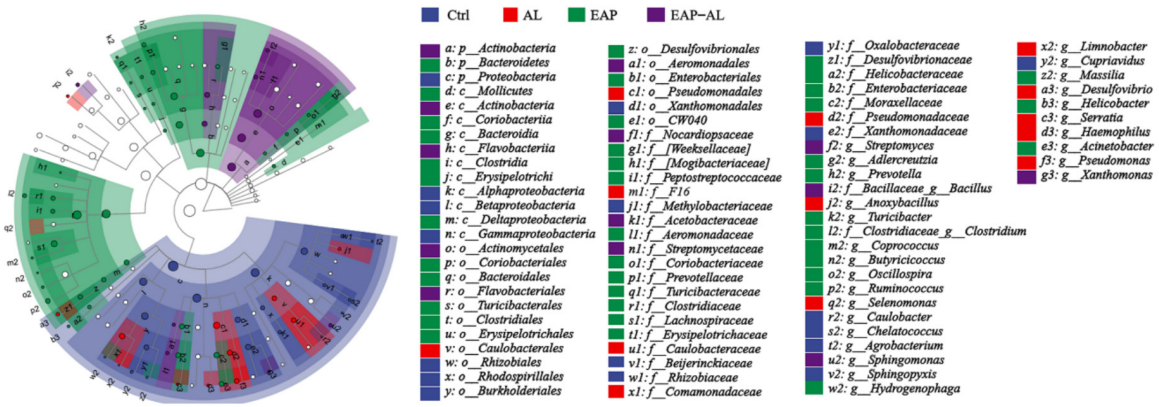

Figure 5. Alcohol promoted the dysbiosis of prostate microbiota profile in EAP rats. The marker species of the prostate microbiota at the different levels by LefSe analysis. The taxonomic branching diagram showed the hierarchical relationship of the main taxa from phylum to genus (from inner circle to outer circle).

groups, including the changes of Bacteriodetes, Firmicutes (Clostridum, and Blautia), and Proteobacteria (Balneimonas) (**Figure 4D**). These findings demonstrated the marker species for alcohol exposure in EAP rats.

Alcohol-induced dysbiosis of the prostate microbiota in EAP rats

The associated network analysis was performed to analyze the similarity of prostate microbiota among four groups. As shown in **Figure 5**, Linear Discriminant Analysis (LDA) with a threshold score of 2 identified key taxa contributing to group-specific microbial structures. At the phylum levels, Proteobacteria were predominant in the Ctrl group, Bacterodietes in the EAP group, and Actinobacteria in the EAP-AL group. At the class level, there were 3 dominant class in Ctrl rats (Alphaproteobacteria, Betaproteobacteria and gammaproteobacterial), 6 in EAP (Mollicute, Coribobacteriia, Bacteroidia, Clostridia, Erysipelotrichi, and Deltaproteobacteria), and 2 in EAP-AL rats (Actinobacteria and Flavobacteriia). A total of 17 prostate microbiota were found in order levels: 4 in Ctrl, 2 in AL, 8 in EAP and 3 in EAP-AL groups. Family level found more than 20 prostate microbiota across all groups, including Methyobacteriaceae in Ctrl rats, F16 in AL rats, Weeksellaceae in EAP rats, and Acetobacteraceae in EAP-AL rats. Meanwhile, we also observed that 28 prostate microbiota were identified at genus level among four groups. Functional profiling using MetagenomeSeq analysis predicted 56 metabolic pathways with significant differences among the four groups, including biosynthesis, degradation/utilization/assimilation, detoxification, generation of precursor metabolite and energy, macromolecule modification, and metabolic cluster (**Figure 6**). Notably, pathways related to amino acid biosynthesis were as follows: cofactor, prosthetic, Group, Electron Carrier, and Vitam Biosythesis, Fatty Acids and Lipid Biosynthesis and Nucleoside and Nucelotide Biosynthesis, Degradation/Utilization/Assimilation for Carbothdrate degradation, Carboxylate degradation, Nucleoside and Nucleotide Degradation, Detoxification for Aantibiotic resistance, and methanol oxidation to carbon dioxide, Generation of precursor metabolite and energy for Electron Transfer, Fermentation, Glycolysis and TCA cycle, Glycan pathways for glycan biosythesis and glycan degradation, and Macromolecule modification for nucleic acid processing and protein modification, and metabolic clusters for O-antigen building blocks biosythesis, pyrimidine deoxyribonucleotide phosphorylation. A total of 51 significantly altered metabolic pathways were identified in the EAP group compared to the Ctrl group, including 28 upregulated and 23 downregulated pathways (**Figure 7A**). Interestingly, in the EAP-AL group compared to Ctrl, 13 pathways (PWY) were upregulated (e.g., PWY-6339, PWY-5860 and PWY-5862), and 19 were downregulated (e.g., PWY0-42, PWY-5747, and PWY-722) (**Figure 7B**). Moreover, pathways such as PWY-7456, PWY-6588, PWY-7210, PWY-7198, PWT-5677, P162-PWY and PWY-5177 were significantly downregulated in the EAP-AL compared to the EAP group (**Figure 7C**).

Additionally, we analyzed the microbial contributions to specific metabolic pathways. The

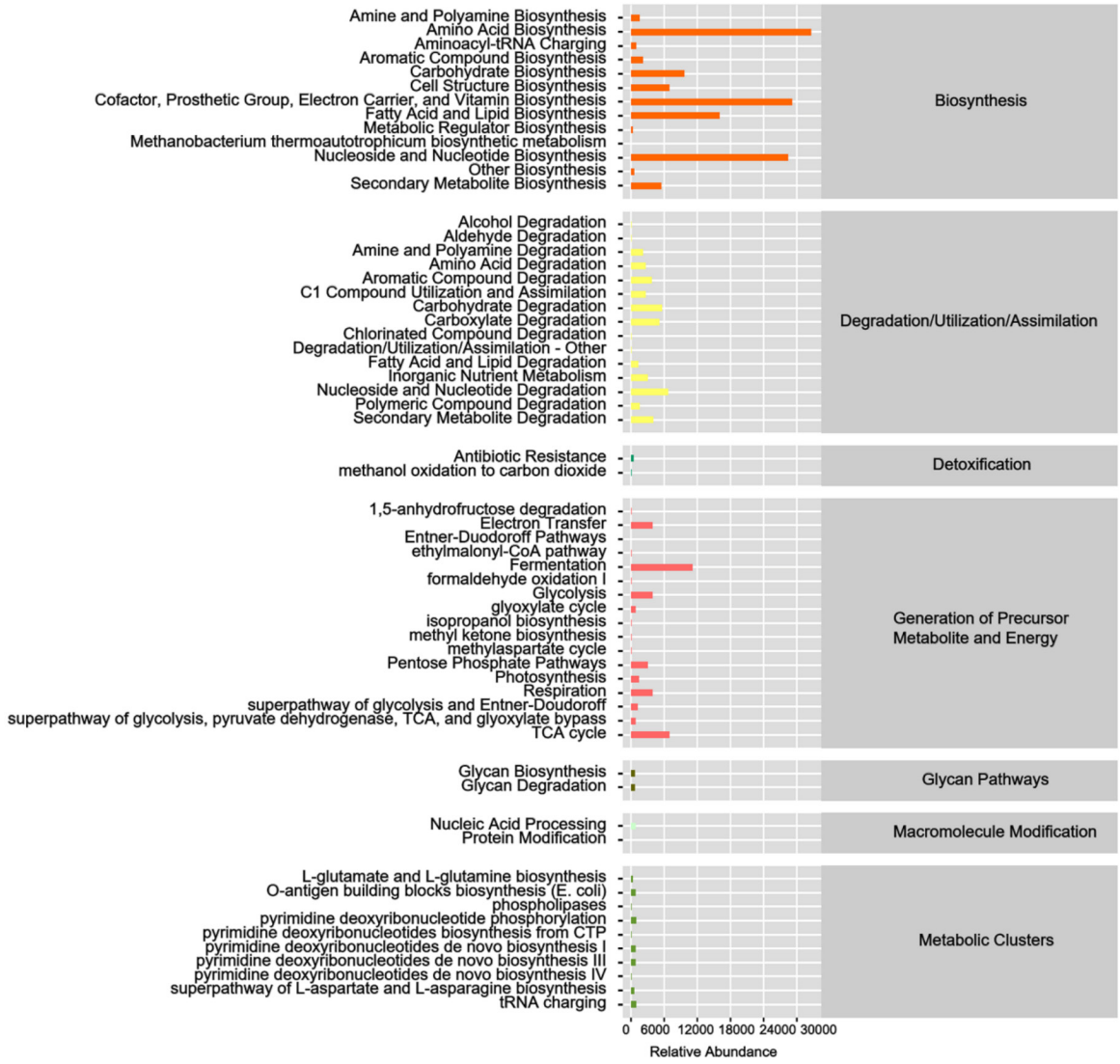

Figure 6. The metabolic pathway analysis by MetagenomeSeq analysis. The relative abundance and function of metabolic pathways among four groups.

composition of prostate microbiota in PWY-722 metabolic pathway was analysis in Ctrl, AL, EAP and EAP-AL groups (**Figure 8A**). In the Ctrl group, PWY-722 were primarily associated with Cupriavidus, Streptomyces, and unidentified-Acetobacteraceae. Cupriavidus, Streptomyces were also strongly correlated with PWY-722 in the AL group. However, in the EAP and EAP-AL groups, PWY-722 was associated with Streptomyces. For PWY-5177, Streptomyces was the main contributor across all groups, with additional contributions from Cupriavidus, unidentified-Xanthomonadaceae, and unidentified-Acetobacteraceae in the Ctrl group; Oscillospira in the AL group; Oscillospira, Pseudomonas, and unclassified-Bacteria in the EAP group (**Figure 8B**). Then, we also analyzed the composition of prostate microbiota in PWY-6339 (**Figure 8C**). Of the four groups, the Ctrl group had the least amount of prostate microbiota. There was a high abundance of Streptomyces, unclassified-Bacteria, unidentified-Clostridiales in the AL group. Interestingly, Streptomyces, Lactobacillus, and unidentified-Clostridiales were also mainly associated with PWY-6339 in the EAP+AL group. Furthermore, we analyzed the PWY-6876 (**Figure 8D**). Streptomyces, Cupriavidus, and unidentified-Xanthomonadaceae were high associated with PWY-6876 in the Ctrl group. Streptomyces and unclassified-Bacteria were the main contributors of PWY-6876 in the AL group. The composition of prostate microbiota

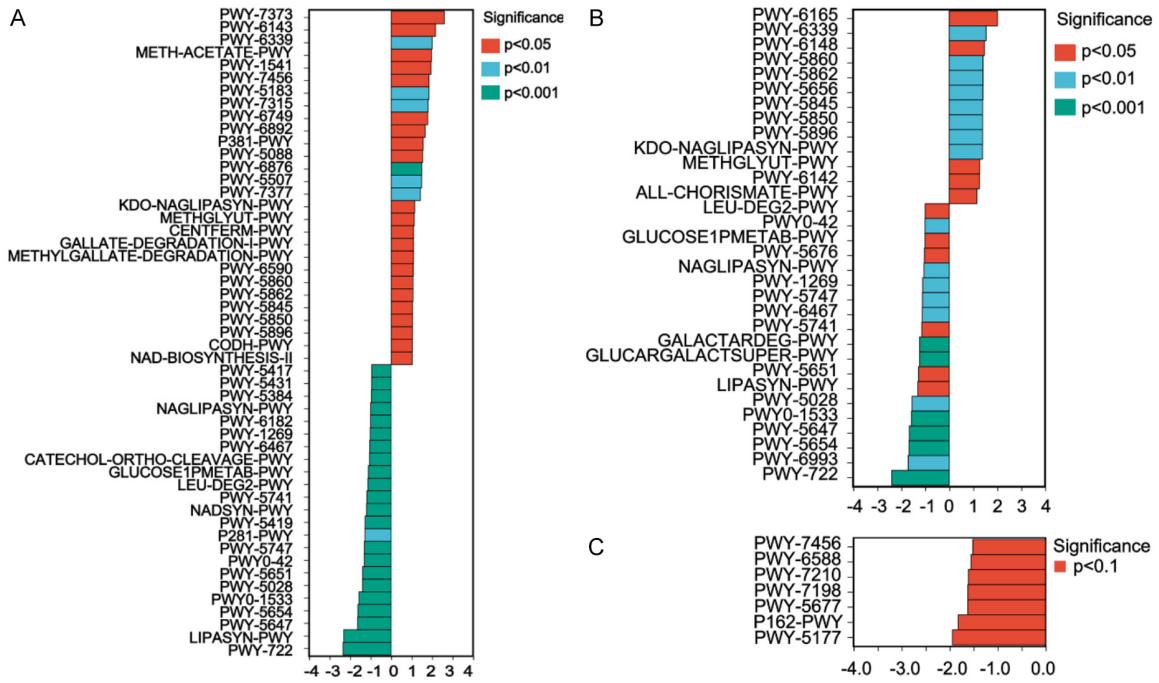

Figure 7. The significant difference analysis of metabolic pathways between two groups. A. Ctrl vs EAP; B. Ctrl vs EAP-AL; C. EAP vs EAP-AL.

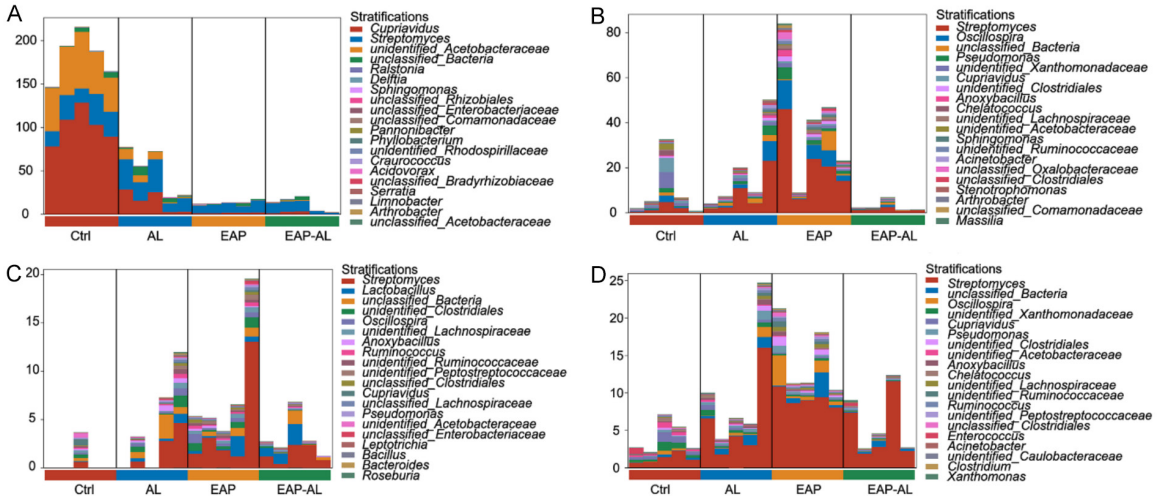

Figure 8. Analysis of the correlation between metabolic pathway and prostate microbiota. The species composition of (A) PWY-722, (B) PWY-5177, (C) PWY-6876, and (D) PWY-6339.

in the EAP group was similar to the AL group. In addition, Oscillospira also strongly correlated with PWY-6876 in the EAP group. In the EAP-AL group, PWY-6876 was mainly regulated by Streptomyces and unclassified-Bacteria.

Discussion

The symptoms of patients with CP/CPPS were influenced by various factors, including lifestyle and dietary habits [11]. While the exact etiology, and pathophysiology remain unclear, clinical practices indicate that alcohol consumption exacerbates CP/CPPS symptoms [28]. The changes in microbiota have been implicated in CP/CPPS [29], and alcohol is known to induce the change in gut microbiota based on the dose and duration [30]. Given the complex interaction between gut and prostate microbiota, alcohol may lead to an imbalance in gut microbiota

and affect prostate health. However, the direct effects of alcohol on prostate microbiota in the context of prostatitis remain unclear.

In this study, we established a rat model of EAP and alcohol exposure to explore the effect of alcohol on prostatitis inflammation and microbial diversity. Our findings showed that alcohol promoted the increase of pro-inflammatory cytokines levels (IL-1β, IL-6, and TNF-α) in EAP rats. Notably, alcohol exposure alone did not significantly alter prostate inflammation scores and factors in Ctrl and AL rats, suggesting that alcohol may exacerbate existing inflammatory conditions rather than initiate them, at least under short-term or specific dosage conditions. This phenomenon could be attributed to the intact epithelial barrier and local immune regulatory mechanisms (e.g., antimicrobial peptide secretion) in the normal prostate, which may resist alcohol-induced microbial translocation or inflammatory triggers. Additionally, the relatively low activity of alcohol-metabolizing enzymes in prostate tissue may result in slower local ethanol metabolism, thereby reducing the risk of direct tissue damage. Furthermore, the alcohol dosage/duration used in this study might not have reached the threshold required to induce significant effects. Using 16S rRNA gene sequencing, we measured the prostate microbial evenness, diversity, and composition. α-diversity and β-diversity analysis indicated significant difference of prostate microbiota in the EAP rats exposed to alcohol (EAP-AL) compared to control, EAP only, and alcohol only groups. More than 1,300 prostate microbiota were identified in the EAP-AL rats, with EAP-AL microorganisms from a variety of genera, including Streptomyces and Oscillospira. Microbiota was correlated with metabolic phenotype [31], and significant alternations were observed in microbiota related to pathways such as biosynthesis, utilization, degradation, assimilation, detoxification, generation of precursor metabolite and energy, glycan pathways, macromolecule modification, and metabolic clusters in the EAP-AL group. Additionally, alcohol changed the composition of the prostate microbiota in metabolic pathways PWY-722 (anti-inflammatory response), PWY-5177 (cell wall synthesis), PWY-6339 (energy metabolism), and PWY-6876 (lipid metabolism) in EAP-AL rats. These findings suggest that alcohol-induced microbiota alterations may contribute to the pathogenesis of prostatitis through multiple metabolic mechanisms.

Alcohol may promote inflammation and suppress the function of the immune system to exacerbate symptoms of prostatitis [32]. Alcohol Inflammatory mediators in the innate immune system distinguish microbes from themselves by identifying conservative microbial structures called PAMPs [33]. Interestingly, Inflammatory bodies were important components of microorganisms, which may lead to the cleavage of precursor IL-1β into its active form IL-1β and promote inflammation [34]. IL-1β had been proven to be a key marker of CP/CPPS [35]. In our study, we found alcohol increased the inflammation response in CP/CPPS rats, but the potential effect was not significant in control rats, which was consistent with previous reports [36]. To further investigate whether alcohol modulates the prostatic microbial community and subsequently influences the inflammatory status of CP/CPPS, we employed bioinformatics analysis to identify differentially abundant microbes in CP/CPPS rats. We found that alcohol significantly altered the microbial diversity in CP/CPPS rat models and disrupted the key metabolic pathways. These findings are consistent with studies showing that alcohol affects multiple metabolic pathways involved in inflammation [37]. Our research demonstrated that alcohol had not only impacted the PWY-722 pathway (anti-inflammatory response) but also affected key pathways such as PWY-5177 (associated with cell wall synthesis), PWY-6339 (tightly linked to energy metabolism), and PWY-6876 (involved in lipid metabolism). Disruptions of these metabolic pathways were closely associated with changes in the host microbiome, highlighting the multifaceted mechanisms through which alcohol influences prostate health. These impaired metabolic pathways could serve as potential biomarkers for monitoring and treating alcohol-related prostatitis. Moreover, we identified key microorganisms associated with these impaired metabolic pathways: Streptomyces in PWY-722, Streptomyces, Oscillospira, Pseudomonas, and unclassified-Bacteria in PWY-5177, Streptomyces, Lactobacillus, and unidentified-Clostridiale in PWY-6339, Streptomyces and unclassified-Bacteria in PWY-6876, revealing a critical role for microbes in this complex metabolic network.

These key microbes and their metabolites may serve as novel biomarkers that could help improve the diagnostic and monitoring accuracy of alcohol-related prostatitis. Importantly, these key microbes and their interaction opened up the possibility for developing therapeutic strategies targeting these microbes, such as probiotic supplementation, antibiotic-targeted therapy, or microbiome dietary interventions, which can be developed in the future, and these strategies may provide new treatment directions for alcohol-related prostatitis.

Our study has several limitations. The influence of alcohol on prostate microbiota, while evident, may be understated due to the limited sample size. Moreover, while we observed metabolic disruptions and microbiota dysbiosis in prostatitis, the underlying molecular mechanisms require further experimental validation. Expanding the sample size and conducting clinical studies will be essential to verify these findings. Furthermore, exploring the effects of varying alcohol dosages and exposure durations on prostatitis progression will provide a more comprehensive understanding.

In summary, our data showed that alcohol exacerbates the dysbiosis in prostate microbiota and alters metabolic phenotypes in EAP rats. Specifically, alcohol modulates the composition of the prostate microbiota in metabolic pathways such as anti-inflammatory response, energy metabolism and lipid metabolism in EAP+AL rats, potentially contributing to the pathological mechanism of prostatitis. These insights may inform the development of targeted therapies for CP/CPPS in individuals consuming alcohol.

Disclosure of conflict of interest

None.

Address correspondence to: Feng Liu, Department of Urology, Shanghai Fengxian District Central Hospital, No. 6600, Nanfeng Road, Shanghai 201499, P. R. China. E-mail: peakliu@alumni.sjtu.edu.cn

References

[1] Zhang J, Liang C, Shang X and Li H. Chronic prostatitis/chronic pelvic pain syndrome: a disease or symptom? Current perspectives on diagnosis, treatment, and prognosis. Am J Mens Health 2020; 14: 1557988320903200.

[2] Rees J, Abrahams M, Doble A and Cooper A; Prostatitis Expert Reference Group (PERG). Diagnosis and treatment of chronic bacterial prostatitis and chronic prostatitis/chronic pelvic pain syndrome: a consensus guideline. BJU Int 2015; 116: 509-525.

[3] Urkmez A, Yuksel OH, Uruc F, Akan S, Yildirim C, Sahin A and Verit A. The effect of asymptomatic histological prostatitis on sexual function and lower urinary tract symptoms. Arch Esp Urol 2016; 69: 185-191.

[4] Liu Y, Mikrani R, Xie D, Wazir J, Shrestha S, Ullah R, Baig MMFA, Ahmed A, Srivastava PK, Thapa KB and Zhou X. Chronic prostatitis/chronic pelvic pain syndrome and prostate cancer: study of immune cells and cytokines. Fundam Clin Pharmacol 2020; 34: 160-172.

[5] Schneider L, Dansranjav T, Neumann E, Yan H, Pilatz A, Schuppe HC, Wagenlehner F and Schagdarsurengin U. Post-prostatic-massage urine exosomes of men with chronic prostatitis/chronic pelvic pain syndrome carry prostate-cancer-typical microRNAs and activate proto-oncogenes. Mol Oncol 2023; 17: 445-468.

[6] Mykoniatis I, Pyrgidis N, Sokolakis I, Sountoulides P, Hatzichristodoulou G, Apostolidis A and Hatzichristou D. Low-intensity shockwave therapy for the management of chronic prostatitis/chronic pelvic pain syndrome: a systematic review and meta-analysis. BJU Int 2021; 128: 144-152.

[7] Singh VK, Yadav D and Garg PK. Diagnosis and management of chronic pancreatitis: a review. JAMA 2019; 322: 2422-2434.

[8] Bataller R, Arab JP and Shah VH. Alcohol-associated hepatitis. N Engl J Med 2022; 387: 2436-2448.

[9] Valverde-López F, Martínez-Cara JG and Redondo-Cerezo E. Acute pancreatitis. Med Clin (Barc) 2022; 158: 556-563.

[10] Zhou T, Im PK, Hariri P, Du H, Guo Y, Lin K, Yang L, Yu C, Chen Y, Sohoni R, Avery D, Guan M, Yang M, Lv J, Clarke R, Li L, Walters RG, Chen Z and Millwood IY; China Kadoorie Biobank Group. Associations of alcohol intake with subclinical carotid atherosclerosis in 22,000 Chinese adults. Atherosclerosis 2023; 377: 34-42.

[11] Bian Z, Jin C, Mo F, Zhang S, Meng J, Zhang M, Zhang L, Chen X, Hao Z, Song Z and Liang C. Dietary habits and lifestyle related to the effectiveness of low-intensity extracorporeal shock wave therapy for chronic prostatitis/chronic pelvic pain syndrome-like symptoms: initial results. Andrologia 2022; 54: e14490.

[12] Zhang LG, Chen J, Meng JL, Zhang Y, Liu Y, Zhan CS, Chen XG, Zhang L and Liang CZ. Ef-

fect of alcohol on chronic pelvic pain and prostatic inflammation in a mouse model of experimental autoimmune prostatitis. Prostate 2019; 79: 1439-1449.
[13] Huang A, Chang B, Sun Y, Lin H, Li B, Teng G and Zou ZS. Disease spectrum of alcoholic liver disease in Beijing 302 hospital from 2002 to 2013: a large tertiary referral hospital experience from 7422 patients. Medicine (Baltimore) 2017; 96: e6163.
[14] Malacco NLSO, Souza JAM, Martins FRB, Rachid MA, Simplicio JA, Tirapelli CR, Sabino AP, Queiroz-Junior CM, Goes GR, Vieira LQ, Souza DG, Pinho V, Teixeira MM and Soriani FM. Chronic ethanol consumption compromises neutrophil function in acute pulmonary aspergillus fumigatus infection. Elife 2020; 23: e58855.
[15] de Timary P, Stärkel P, Delzenne NM and Leclercq S. A role for the peripheral immune system in the development of alcohol use disorders? Neuropharmacology 2017; 122: 148-160.
[16] Salachan PV, Rasmussen M, Fredsøe J, Ulhøi B, Borre M and Sørensen KD. Microbiota of the prostate tumor environment investigated by whole-transcriptome profiling. Genome Med 2022; 14: 9.
[17] Kustrimovic N, Bombelli R, Baci D and Mortara L. Microbiome and prostate cancer: a novel target for prevention and treatment. Int J Mol Sci 2023; 24: 151.
[18] Siddiqui MT and Cresci GAM. Microbiota reprogramming for treatment of alcohol-related liver disease. Transl Res 2020; 226: 26-38.
[19] Thomas S, Dunn CD, Campbell LJ, Strand DW, Vezina CM, Bjorling DE, Penniston KL, Li L, Ricke WA and Goldberg TL. A multi-omic investigation of male lower urinary tract symptoms: potential role for JC virus. PLoS One 2021; 16: e0246266.
[20] Marschalkó M and Ambrus L. Characteristics and physiologic role of female lower genital microbiome. Orv Hetil 2023; 164: 923-930.
[21] Dong YH, Fu Z, Zhang NN, Shao JY, Shen J, Yang E, Sun SY, Zhao ZM, Xiao A, Liu CJ and Li XR. Urogenital tract and rectal microbiota composition and its influence on reproductive outcomes in infertile patients. Front Microbiol 2023; 14: 1051437.
[22] Chen J, Zhan C, Zhang L, Zhang L, Liu Y, Zhang Y, Du H, Liang C and Chen X. The hypermethylation of Foxp3 promoter impairs the function of treg cells in EAP. Inflammation 2019; 42: 1705-1718.
[23] Liu F, Xu X, Wang Z and Wu P. Abnormal prostate microbiota composition is associated with experimental autoimmune prostatitis complicated with depression in rats. Front Cell Infect Microbiol 2022; 12: 966004.
[24] Risbud RD, Breit KR and Thomas JD. Early developmental alcohol exposure alters behavioral outcomes following adolescent re-exposure in a rat model. Alcohol Clin Exp Res 2022; 46: 1993-2009.
[25] Nguyen TMT, Steane SE, Moritz KM and Akison LK. Prenatal alcohol exposure programmes offspring disease: insulin resistance in adult males in a rat model of acute exposure. J Physiol 2019; 597: 5619-5637.
[26] Zhang K, Wang A, Zhong K, Qi S, Wei C, Shu X, Tu WY, Xu W, Xia C, Xiao Y, Chen A, Bai L, Zhang J, Luo B, Wang W and Shen C. UBQLN2-HSP70 axis reduces poly-Gly-Ala aggregates and alleviates behavioral defects in the C9ORF72 animal model. Neuron 2021; 109: 1949-1962, e6.
[27] Tabatabaei MS and Ahmed M. Enzyme-linked immunosorbent assay (ELISA). Methods Mol Biol 2022; 2508: 115-134.
[28] Zhang Z, Li Z, Yu Q, Wu C, Lu Z, Zhu F, Zhang H, Liao M, Li T, Chen W, Xian X, Tan A and Mo Z. The prevalence of and risk factors for prostatitis-like symptoms and its relation to erectile dysfunction in Chinese men. Andrology 2015; 3: 1119-1124.
[29] Bajic P, Dornbier RA, Doshi CP, Wolfe AJ, Farooq AV and Bresler L. Implications of the genitourinary microbiota in prostatic disease. Curr Urol Rep 2019; 20: 34.
[30] Leclercq S, Stärkel P, Delzenne NM and de Timary P. The gut microbiota: a new target in the management of alcohol dependence? Alcohol 2019; 74: 105-111.
[31] He J, Xu S, Zhang B, Xiao C, Chen Z, Si F, Fu J, Lin X, Zheng G, Yu G and Chen J. Gut microbiota and metabolite alterations associated with reduced bone mineral density or bone metabolic indexes in postmenopausal osteoporosis. Aging (Albany NY) 2020; 12: 8583-8604.
[32] Dukić M, Radonjić T, Jovanović I, Zdravković M, Todorović Z, Kraišnik N, Arandelović B, Mandić O, Popadić V, Nikolić N, Klašnja S, Manojlović A, Divac A, Gačić J, Brajković M, Oprić S, Popović M and Branković M. Alcohol, inflammation, and microbiota in alcoholic liver disease. Int J Mol Sci 2023; 24: 3735.
[33] Ray SK, Macoy DM, Kim WY, Lee SY and Kim MG. Role of RIN4 in regulating PAMP-triggered immunity and effector-triggered immunity: current status and future perspectives. Mol Cells 2019; 42: 503-511.
[34] Qi J, Yan X, Li L, Qiu K, Huang W and Zhou Z. CXCL5 promotes lipotoxicity of hepatocytes through upregulating NLRP3/Caspase-1/IL-1β signaling in Kupffer cells and exacerbates nonalcoholic steatohepatitis in mice. Int Immunopharmacol 2023; 123: 110752.
[35] Wong L, Done JD, Schaeffer AJ and Thumbikat P. Experimental autoimmune prostatitis induc-

es microglial activation in the spinal cord. Prostate 2015; 75: 50-59.

[36] Yamaguchi M, Yoshiike K, Watanabe H and Watanabe M. The marine factor 3,5-dihydroxy-4-methoxybenzyl alcohol suppresses cell growth, inflammatory cytokine production, and NF-κB signaling-enhanced osteoclastogenesis in in vitro mouse macrophages RAW264.7 cells. Curr Mol Med 2024; 24: 813-825.

[37] Du HX, Yue SY, Niu D, Liu XH, Li WY, Wang X, Chen J, Hu DK, Zhang LG, Guan Y, Ji DX, Chen XG, Zhang L and Liang CZ. Alcohol intake exacerbates experimental autoimmune prostatitis through gut microbiota driving cholesterol biosynthesis-mediated Th17 differentiation. Int Immunopharmacol 2024; 139: 112669.